Magnetic behavior and resistivity of the domain-wall junction GdFe 1000 Å /TbFe/GdFe 500 Å

S Mangin, G. Marchal, C. Bellouard, W. Wernsdorfer, B. Barbara

Magnetic behavior and resistivity of the domain-wall junction GdFe(1000 Å)/TbFe/GdFe(500 Å)

S. Mangin
Laboratoire de Magnétisme Louis Néel, CNRS, BP166, 38042 Grenoble cedex 9, France
and Laboratoire de Physique des Matériaux, Université Henri Poincaré-Nancy I, BP 239, 54506 Vandoeuvre les Nancy cedex, France

G. Marchal and C. Bellouard
Laboratoire de Physique des Matériaux, Université Henri Poincaré-Nancy I, BP 239, 54506 Vandoeuvre les Nancy cedex, France

W. Wernsdorfer and B. Barbara
Laboratoire de Magnétisme Louis Néel, CNRS, BP166, 38042 Grenoble cedex 9, France
(Received 6 August 1997; revised manuscript received 14 January 1998)

A GdFe/TbFe/GdFe trilayer constitutes a magnetic nanostructure: the domain wall junction. With this device, we studied the propagation of 180° domain walls from one GdFe layer to the other, through a single planar defect (the thin TbFe layer) that acts as an artificial energy barrier. Before crossing the energy barrier, by thermal activation, due to the applied magnetic field, the domain walls are compressed against the TbFe layer. Nucleation, compression, and propagation phenomena of 180° domain walls are presented. The behavior of domain walls is followed from the electrical resistivity of the sample. A parallel between the domain-wall decompression and the exchange biasing problem in ferromagnetic/antiferromagnetic bilayers is proposed. [S0163-1829(98)01629-4]

I. INTRODUCTION

The propagation of magnetic domain walls in ferromagnetic or ferrimagnetic materials is known to be of considerable importance for magnetic applications. Indeed, depending on the ability of its domain walls to move, a material is classified among the hard or among the soft magnetic materials.[1] Moreover, the propagation of the domain walls is of great interest for theoreticians studying the dynamics of assemblies of spins: at high temperature, where the thermal activation plays an important role, or at low temperature, where quantum effects could arise.[2–5] Usually, domain walls interact with magnetic or nonmagnetic defects (precipitates, grain boundaries, etc.). These defects act as potential wells or as potential barriers that the domain walls have to cross to travel inside the material and to reverse the magnetization. However, in most of the usual macroscopic samples, the defects are very complex and present a large distribution of shape and of size, which makes the analysis very complicated.

In a recent paper, Gunther and Barbara proposed a device called a domain-wall junction (DWJ),[4] which can be considered as a model system suitable for the study of the interaction between a 180° magnetic domain wall and a well-defined potential-energy barrier. This device consists of a ferromagnetic or ferrimagnetic trilayer system, with an in-plane uniaxial anisotropy, in which a layer of hard magnetic material separates two layers of soft magnetic material. As the potential energy per surface unit of the domain wall is simply the usual domain-wall energy $\gamma = 4\sqrt{AK}$, where K is the uniaxial anisotropy constant and A is the exchange stiffness, the hard magnetic material, which presents the larger anisotropy constant, acts as a potential barrier [Fig. 1(a)]. Therefore, to move from one layer of soft magnetic material to the second one, the domain wall has to cross the hard magnetic material and the associated potential-energy barrier.

In fact, the motion of the domain wall is achieved by the application of an external magnetic field that produces a magnetic pressure on the domain wall.[1] The displacement induced by the magnetic pressure is such that the magnetic domains orientated parallel to the field grow. As shown in the potential-energy diagram of Fig. 1(b), the magnetic field adds a linear Zeeman contribution $-2M_S H\ x$ to the zero-field potential.[4]

The second effect of the magnetic field is to reduce the height of the potential barrier due to the hard magnetic ma-

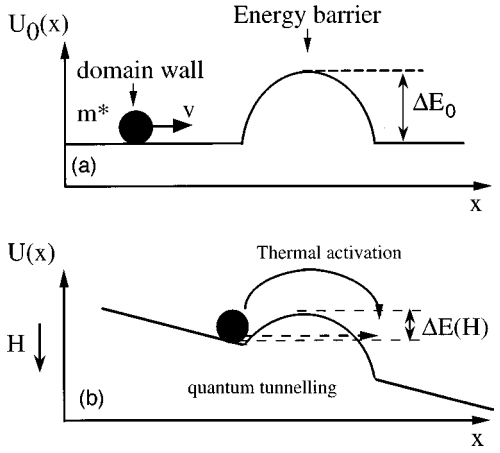

FIG. 1. Potential barrier created by a layer of hard magnetic material deposited between two layers of soft magnetic material. (a) under zero magnetic field, (b) with an applied magnetic field. The black ball represents the domain wall, m^* is its mass, and v its velocity. ΔE_0 is the height of the potential barrier in zero field. When the field is applied, a $-2M_S H\ x$ component is added and the height of the barrier is reduced.

terial [Fig. 1(b)]. The aim of the study of the DWJ is the determination of the field and temperature conditions under which the potential barrier is crossed and by which mechanism: thermal activation or quantum tunneling.

In a preliminary paper,[6] we proposed a DWJ system made of a very thin layer of amorphous $Tb_{45}Fe_{55}$ alloy deposited between two layers of $Gd_{62}Fe_{38}$ ferrimagnetic amorphous alloy.[7] The amorphicity of the layers generates a structural continuity of the sample and prevents structural defects in the form of grain boundaries, which could generate parasitic potentials. The structural continuity is all the better that Tb and Gd atoms are very similar (same size, same chemical behavior) and form with isomorphic amorphous alloys iron.[8] The large anisotropy of terbium compared to that of gadolinium (the second-order anisotropy constant K of terbium is three orders of magnitude larger than that of gadolinium[9]) makes the TbFe layer a potential barrier for a domain wall that has to move from the first GdFe layer to the second one.

The compositions of the alloys were chosen according to several criteria. First of all, the alloys had to be amorphous. Then, they had to exhibit a large magnetization density for a better sensitivity in magnetic measurements. It was also preferable to avoid alloy compositions presenting a compensation temperature, which could have added complications. Finally, from the data reported by Hansen *et al.*,[10] we chose the compositions $Gd_{62}Fe_{38}$ and $Tb_{45}Fe_{55}$, which exhibit close Curie temperatures and thus exchange coupling constants of the same order of magnitude. Nevertheless, the composition of the alloys is probably not critical and a change of the compositions of the alloys should not significantly alter the results.

In this paper, we confirm our first data[6] and show the efficiency of the GdFe/TbFe/GdFe domain-wall junction. We present in detail the mechanisms of nucleation, compression, propagation, double compression, and annihilation of the domain walls, as deduced from the magnetization measurements and confirmed by resistivity measurements. The very demonstrative resistivity data displayed in this paper are obtained from a single-domain wall.

We also present a diagram indicating at which temperature and under which magnetic field the energy barriers generated by very thin TbFe layers (from 3 to 9 Å) are crossed by the domain walls. These very small thicknesses of the hard magnetic layers should classify the GdFe/TbFe/GdFe DWJ in the regime II-b of the classification proposed by Gunther and Barbara.[4] In that regime, the thickness of the hard magnetic layer as well as s, the width of the transition region between the two materials, are smaller than the width δ of the domain wall.

Finally, we focus on the compression of the domain walls against the TbFe layers that precedes the crossing of the barriers. This stage is probably typical of systems in which the domain-wall energy of the hard magnetic layer is very high. A parallel between the domain-wall compression and the exchange biasing problem is proposed.

II. EXPERIMENTAL PROCEDURE

The data presented in this study have been collected from GdFe/TbFe/GdFe samples, in which the thicknesses of the GdFe layers are $e_1 = 1000$ Å, $e_2 = 500$ Å, and the thickness of the TbFe layer ranges from $e = 3$ Å to $e = 15$ Å.

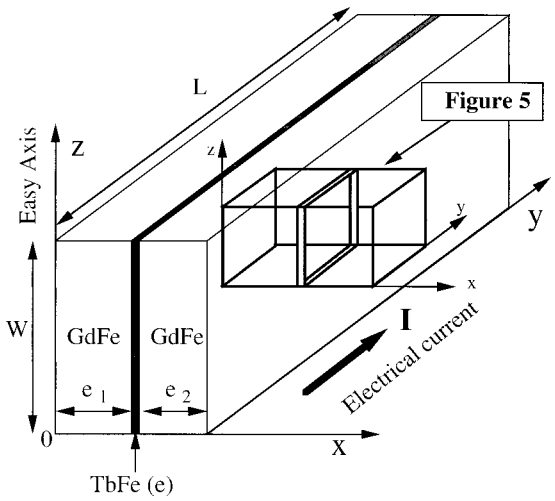

FIG. 2. General view of the sample. The length L of the sample is 2 cm and its width is 0.5 cm. The easy magnetization axis is along $0z$. The slab ''Fig. 5'' will be enlarged for the description of the magnetic configurations in Fig. 5. The electrical current flowing along $0y$ will be used to measure the resistance of the sample in the transverse geometry (see Sec. IV).

The alloys were obtained by high vacuum coevaporation of the elements from separate crucibles. The deposition rates were monitored by quartz oscillating systems, previously calibrated by optical methods.[11] The compositions of the alloys were subsequently checked by x-ray analysis and were found within 1% of the nominal values. As the quartz oscillators are sensitive to the mass, the thicknesses of the layers were deduced from the density of the amorphous alloys, in the same way as in Ref. 12. The substrates were glass plates on which 100 Å silicon buffer layers were deposited at 150 °C just before the cooling down of the substrates, which were kept at 77 K during the coevaporation process. The pressure in the chamber was maintained at 10^{-8} Torr during the deposition of the alloys. The amorphicity of the alloys was checked by electron microscopy and observation of the typical diffuse rings consistent with the interference functions of rare-earth transition metals and amorphous alloys.[13]

The magnetization measurements were performed with a conventional superconducting quantum interference device magnetometer. Each of the curves shown in Figs. 3, 4, and 6 were obtained after cooling down the sample from 100 K to the measurement temperature under a 1000 Oe magnetic field applied along the easy axis of magnetization. With this procedure, the magnetization was kept saturated along the cooling field, even after canceling the field. The magnetization curves presented below were obtained while increasing the field in the direction antiparallel to the cooling field. Electrical resistivity measurements were performed with a four-point method in a magnet-equipped cryostat in the same way as measurements reported in Ref. 14.

A general view of a sample is pictured in Fig. 2. The length L of the sample is 2 cm and its width is 0.5 cm. $0x$ is perpendicular to the plane of the sample and, as shown below, the easy magnetization axis is along $0z$. In the following, the slab ''Fig. 5'' will be enlarged for the description of the magnetic configurations. The electrical current flowing

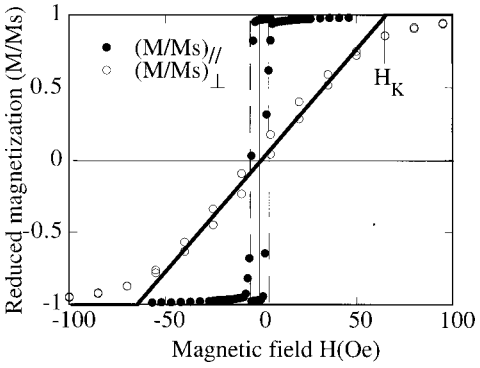

FIG. 3. Hysteresis loops of a single 1000 Å GdFe layer measured at 10 K. The field is applied along the easy axis $(M/M_S)_{\parallel}$ and perpendicularly to the easy axis $(M/M_S)_{\perp}$. H_K is the saturation field of the Stoner and Wohlfarth model (Refs. 15 and 16).

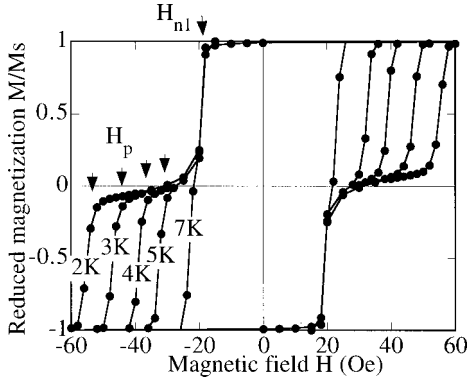

FIG. 4. Hysteresis loops collected from a GdFe (1000 Å)/TbFe(3 Å)/GdFe(500 Å) sample at different temperatures. The first parts (negative fields) of the loops have been obtained after cooling the sample under a 1000 Oe field. The second parts have been collected after the application of a -1000 Oe field at the measurement temperature. H_{n1} is the nucleation field for the GdFe(1000 Å) layer. H_p is the propagation field (passage of the domain wall through the potential barrier).

along $0y$ will be used to measure the resistivity of the sample in the transverse geometry (see Sec. IV).

III. MAGNETIC BEHAVIOR

A. In-plane anisotropy axis

First of all, the presence of an uniaxial anisotropy axis in the plane of the sample is necessary for the creation of 180° domain walls. The occurrence of such an axis is clearly demonstrated in Fig. 3 that represents two hysteresis loops collected from a single $Gd_{62}Fe_{38}$(1000 Å) layer with, in both cases, the magnetic field applied in the plane of the sample. The field was applied either along the easy axis ($M_{\parallel}$ loop) or perpendicularly to the easy axis ($M_{\perp}$ loop). Such a behavior is quite consistent with the classical Stoner and Wohlfarth model of uniform rotation:[15] the $M_{\parallel}$ hysteresis loop is rectangular, whereas the $M_{\perp}$ hysteresis loop is linear from $-H_K$ to $+H_K$, where H_K is the anisotropy field. H_K is at the intercept of the linear part and of the saturation magnetization (for a review, see, for example, Ref. 16). As a matter of fact, the evaporation of Gd and Fe from two separate crucibles positioned symmetrically with respect to the substrate leads spontaneously to the occurrence of an easy magnetization axis in the plane of the sample. The anisotropy axis is perpendicular to the vertical plane containing the sources.[17] The existence of such an anisotropy axis has been observed with different preparation procedures.[18]

Following Stoner and Wolfarth, the uniaxial anisotropy constant K can be deduced from the anisotropy field H_K by the relation $K=M_S H_K/2$,[15,16] where M_S is the saturation magnetization. From very low field (0.25 Oe) ac susceptibility measurements, the Curie temperature of the $Gd_{62}Fe_{38}$ (1000 Å) sample has been found to be 325 K, which is very close to the value given by the reference paper of Hansen *et al.*[10] for this composition. From these authors, the saturation magnetization M_S is close to 1400 emu/cm^3, which has been checked with an accuracy of 5%. With H_K close to 70 Oe, the uniaxial anisotropy constant can be estimated to $K=4.9\ 10^4$ erg/cm^3. In fact, the 180° domain wall is due to the competition between the exchange and the uniaxial anisotropy energies. As a result of this competition, the thickness of the domain wall is given by $\delta=\pi\sqrt{A/K}$, where the exchange stiffness constant A is related to the usual exchange constants J_{GdGd}, J_{GdFe}, and J_{FeFe} by a relation given for the ferrimagnetic amorphous alloys by Hasegawa[19] and Mimura *et al.*[20] Using the exchange constants published by Hansen *et al.*,[10] and the interatomic distance given by Cargill,[21] the exchange stiffness constant A of the $Gd_{62}Fe_{38}$ amorphous alloy can be estimated to 15×10^{-8} erg/cm. In order to evaluate K, we used the Nimura relation with $n_{\mathrm{Gd}}=3$ and $n_{\mathrm{Fe}}=2$. From these A and K values, the domain-wall thickness in the GdFe samples is evaluated to about 650 Å. This value has to be considered as an estimate at $\pm10\%$. It depends on several parameters that are very difficult to obtain with accuracy. They are deduced from a mean-field approximation and require the evaluation of the Curie temperature of a lot of amorphous alloys. More significant will be the values determined below from the compression of the domain wall.

B. Nucleation and propagation

Magnetization data collected at different temperatures from a GdFe(1000 Å)/TbFe(3 Å)/GdFe(500 Å) sample are shown in Fig. 4. When the temperature is lower than 7 K, each curve exhibits two magnetization steps. The first step occurs at a field $H_{n1}\approx18$ Oe, almost independent of the temperature, where the magnetization drops from the saturation magnetization M_S to a value slightly larger than zero. The second step occurs at a field $H_p(T)$, where the magnetization falls to $-M_S$. In contrast to H_{n1}, $H_p(T)$ is strongly temperature dependent and increases when the temperature decreases. Between the two steps, the magnetization exhibits a slow decrease on a kind of plateau.

As it will be justified in the next sections from the amplitudes of the magnetization drops and from the behavior of the electrical resistivity, the interpretation of the two steps and of the intermediate decrease of magnetization is sketched in Fig. 5 (part of Fig. 2). In these figures, each arrow is representative of the magnetization of a plane parallel to the surface $(0y,0z)$ of the sample. In each plane referred by its position x, all the magnetic moments are supposed to be

parallel to each other and oriented along the arrow representative of the magnetization of the plane. They form an angle $\theta(x)$ with the direction $0y$. $0x$ is the axis along which the domain wall propagates. However, it is likely that the magnetic moments do not rotate in the same way along the $0x$ direction in the whole sample. There are certainly parts of the sample in which the magnetic moments turn clockwise along $0x$, whereas in other parts they turn anticlockwise, which makes that the θ angle is in fact $+\theta(x)$ in some parts of the sample and $-\theta(x)$ in other parts. At the present time, we have no information on these parts which turn out to constitute ''in-plane domains'' but we believe that they are large enough to neglect the defects that should occur at their boundaries. In the following, we will forget the ''in-plane domains'' and the only domain wall we will consider is that which is parallel to the plane of the sample and that propagates along $0x$. We will describe the data as if an unique domain wall is present in the whole sample although it is likely that ''identical'' domain walls move simultaneously and in the same way (except for the chirality) inside each ''in-plane domain.''

Figure 5(a) represents the saturated magnetization along the direction of the cooling field. This saturated configuration is maintained until the field H_{n1} is applied in the direction opposite to the cooling field. The drop of magnetization at H_{n1} corresponds to the nucleation of a magnetic domain in the thicker GdFe(1000 Å) layer. The reversal of the magnetization starts from the outer surface but it is blocked by the TbFe layer [Fig. 5(b)]. The slow continuous decrease of the magnetization between H_{n1} and H_p is attributed to the ''compression'' of the domain wall against the TbFe layer [Fig. 5(c)]. It is the result of the magnetic pressure on the domain wall, which is blocked on its other side by the magnetization of the TbFe layer, stuck itself by its very strong anisotropy. The second drop of the magnetization, which occurs at $H_p(T)$, corresponds to the crossing of the potential barrier by the domain wall. The domain wall first reverses the magnetization of the TbFe layer and then that of the GdFe(500 Å) layer [Fig. 5(d)]. H_p is called the ''propagation field.'' Beyond H_p, the magnetization is completely reversed [Fig. 5(f)]. We notice that, when the temperature is larger (7 K), the magnetization switches from $+M_S$ to $-M_S$ at a field referred as H_{c1}. At this temperature, the TbFe layer seems to be inefficient, which is consistent with the fact that, as it will be shown below, the crossing of the barrier is a thermal activated process.

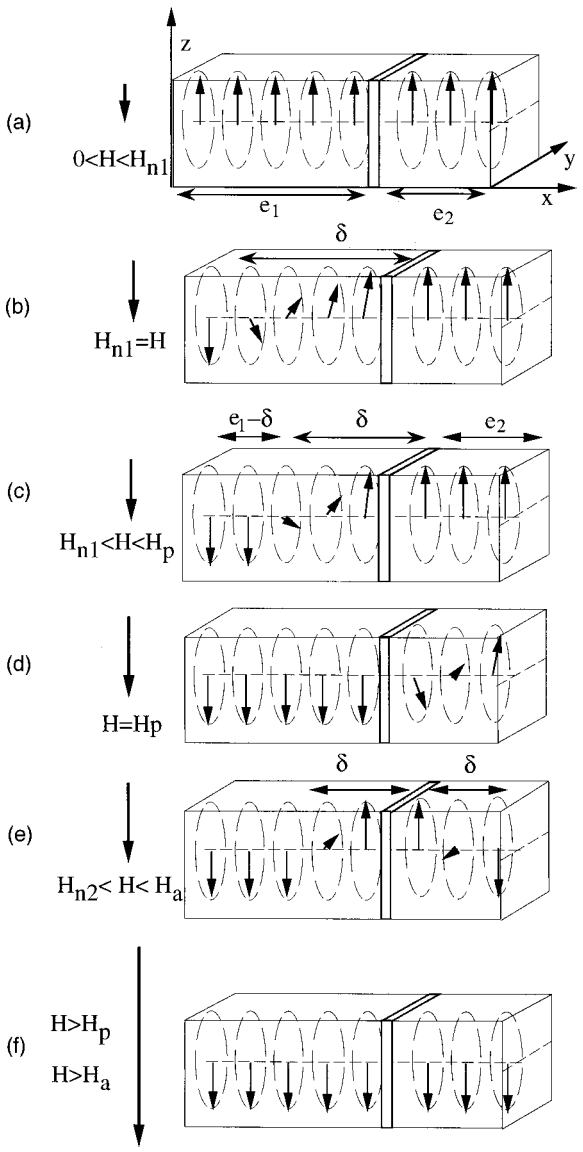

FIG. 5. Modelized magnetization configurations in the trilayer: (a) For an applied magnetic field H, $0<H<H_{n1}$; the magnetization of the sample is saturated. (b) At $H=H_{n1}$ a domain wall is created in the thicker GdFe layer. It is stopped by the TbFe layer. (c) For $H_{n1}<H<H_p$ the domain wall is compressed against the TbFe layer. (d) At $H=H_p$ the TbFe layer magnetization is reversed and the domain wall propagates into the thinner GdFe layer. (e) At $H=H_{n2}$ a second domain wall is nucleated in the thinner GdFe layer. (f) Beyond H_p or H_a the magnetization is completely reversed.

C. Double compression and annihilation

With the same procedure, hysteresis loops have been collected from the GdFe(1000 Å)/TbFe(9.5 Å)/GdFe(500 Å) trilayer (Fig. 6). In the temperature range from 30 to 50 K, the same magnetization behavior as above is observed, with two steps at $H_{n1}\approx 18$ Oe and at $H_p(T)$. Above $T=50$ K, there is an unique step, where the magnetization switches from M_S to $-M_S$ as in the GdFe(1000 Å)/TbFe(3 Å)/GdFe(500 Å) sample above $T=7$ K. The comparison between Figs. 4 and 6 shows that the propagation field is translated towards the highest temperatures when the thickness of the TbFe layer increases.

However, below 20 K, the ''compression'' stage does not end at $H_p(T)$ by a full drop of the magnetization to $-M_S$. There is instead a limited drop of the magnetization at a field H_{n2} close to 60 Oe. This limited drop is followed by another slow decrease of the magnetization, which finally ends by a more rapid decrease of the magnetization to $-M_S$ at a field $H_a(T)$.

We attribute the step occurring at H_{n2} to the nucleation of a second domain wall in the thinner GdFe(500 Å) layer [Fig. 5(e)] and to the propagation of this new domain wall up to the TbFe layer. As it will be explained below, the nucleation of magnetic domains and the corresponding nucleation fields

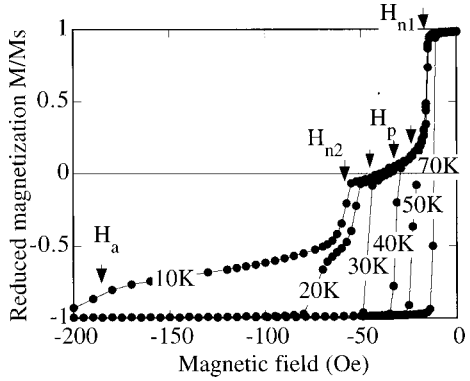

FIG. 6. Hysteresis loops from the GdFe(1000 Å)/TbFe(9.5 Å)/GdFe(500 Å) sample at different temperatures. The measurements were performed after cooling down the sample under a 1000 Oe magnetic field. Only the first part of the cycles has been presented. H_{n2} is the nucleation field for the GdFe(500 Å) layer. H_a is the annihilation field.

are related to the thickness of the GdFe layers. The thicker the layer, the higher the nucleation field. After the second nucleation, the two domain walls are simultaneously compressed against the TbFe layer, which results in a slow decrease of the magnetization with the increase of the field (''double-compression stage'').

Here it is important to emphasize that without the nucleation delay in the thinner GdFe layer ($H_{n2} > H_{n1}$), we never could have observed the propagation of the domain wall through the TbFe layer. The asymmetry of the trilayer system, with two different thicknesses of the GdFe layers, is necessary for the device to operate.

Finally, the last drop of the magnetization is related to the reversal of the TbFe layer magnetization, which occurs with the annihilation of the domain walls at a field $H_a(T)$, the so-called annihilation field. H_a is not as well defined as the other characteristic fields and the transition spreads out on several Kelvin. It is about 80 Oe at 20 K and 180 Oe at 10 K. These fields are relatively high and we can point out the unexpected stability of the configuration of Fig. 5(e) where the TbFe layer is squeezed between two domain walls. Indeed, under the pressure of two domain walls on each side of it, the magnetization of the TbFe layer should switch very easily. This is no longer true if the domain walls tend to rotate the magnetization of the TbFe layer in opposite directions (clockwise and anticlockwise) and as a consequence cancel each other. A first explanation to this high stability would be that the domain walls located on each side of the TbFe layer are systematically of opposite chirality (in all the ''in-plane domains''). It could be due to the effect of the dipolar fields of the first layer, in which domains are already present, on the second one, in which the nucleation is taking place. A second possibility would be that the shape and the distribution of the ''in-plane domains'' in the two GdFe layers are uncorrelated. There are some places where the chiralities of the domain walls located on each part of the TbFe layer would be opposite and some places where they would be identical. The parts where the chiralities would be opposite would maintain strongly the magnetization of the TbFe along the direction of the cooling field.

IV. ELECTRICAL BEHAVIOR

A. The anisotropy of magnetoresistance

It is now well known that the magnetic state of a material can significantly contribute to its electrical resistivity via several different effects. In return, the electrical resistivity can be used to determine or confirm the magnetic structure of a sample.[22]

In this section, we show how the variation of the electrical resistance of the sample with the field allowed us to ascertain that the magnetic configurations sketched in Fig. 5 represent the actual magnetization processes, giving rise to the behavior reported in Figs. 4 and 6. For this purpose, we took advantage of the significant anisotropy of magnetoresistance (AMR) of iron, which has been interpreted by Smit[23] and Fert.[24] As shown by these authors, the resistivity of the transition metals and of their alloys depends significantly on the angle between the direction of the magnetization and the direction of the electrical current used to measure the resistivity. The resistivity is enhanced and equal to $\rho_{\parallel}$ when the electrical current is parallel to the magnetic moments and, at the opposite, it is reduced and equal to $\rho_{\perp}$ when it is perpendicular. Finally, when in an homogeneously magnetized transition metal sample, the angle between the magnetic moments and the electrical current is θ, the resistivity can be expressed as $\rho(\theta) = \rho_{\perp} + \Delta\rho \cos^2\theta$ where $\Delta\rho = \rho_{\parallel} - \rho_{\perp}$.[22] In pure iron, the order of magnitude of $(\rho_{\parallel} - \rho_{\perp})/\rho$ is about 0.5%.[23]

In the following, we will refer to the geometry in which the electrical current flows along the direction of the applied magnetic field (parallel or antiparallel) as parallel and to the geometry in which the electrical current and the magnetic field (always applied along the easy magnetic axis $0z$ in the plane of the sample) are perpendicular as transverse (the transverse geometry is that represented in Fig. 2). This technique permits for example the determination of the coercitive field of thin films, with the occurrence of peaked maxima (in the parallel geometry) or of peaked minima (in the transverse geometry).[25,26] The occurrence of these peaks expresses that, at the coercitive field, a maximum number of spins are oriented rather perpendicularly to the magnetic field. This technique was recently used to show the aligned and twisted phases in GdFe multilayers.[14] It was possible to detect the magnetic field at which the iron moments leave the field direction and exhibit a spin-flop-like transition.

The resistance data presented in this section have been collected from GdFe(1000 Å)/TbFe(15 Å)/GdFe(500 Å) samples. Golden electrodes have been deposited on the glass substrate prior the elaboration of the sample. The orientation of the substrate during the deposition of the sample had been chosen for the easy magnetization axis to be parallel (parallel geometry) or perpendicular (transverse geometry) to the current flow during the electrical measurement. As above, the magnetic field is always applied in the direction of the easy axis (direction $0z$ of Figs. 2 and 5), whereas the current flows along the direction $0y$. The data presented in Figs. 7(a) and 7(b) show the relative variation of the resistance in the transverse geometry (see Fig. 2). The data have been normalized to the resistance value measured in the saturated state.

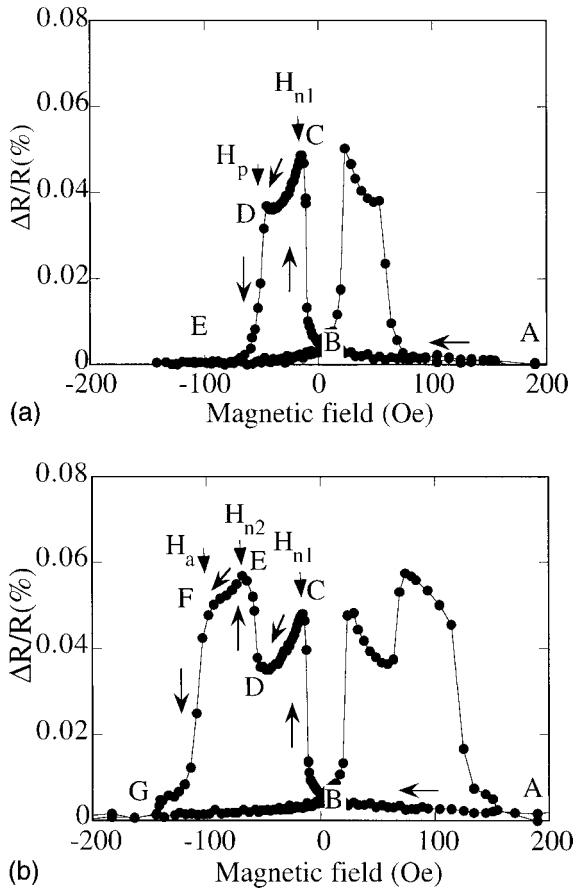

FIG. 7. Evolution at 60 K (a) and at 30 K (b) of the resistance of a GdFe(1000 Å)/TbFe(15 Å)/GdFe(500 Å) sample with the magnetic field applied along the easy axis, perpendicularly to the electrical current (see Fig. 2). The first parts (negative field) have been obtained after cooling down the sample under a 1000 Oe field. The second part (quite symmetrical about the vertical axis) has been obtained after the application of a 1000 Oe field at the measurement temperature. The notation H_{n1}, H_p, H_{n2}, and H_a is the same as in Figs. 4 and 6.

Because the TbFe thickness is larger in this sample than in samples presented above (Figs. 4 and 6), the different magnetization processes are shifted to higher temperatures.

B. Nucleation and propagation

The field dependence of the electrical resistance measured at 60 K in the transverse geometry after the cooling under a 1000 Oe field is shown in Fig. 7(a). At point A, the electrical resistance is minimum: all the magnetic moments are parallel to the magnetic field and thus, because of the transverse geometry, the magnetization is perpendicular to the electrical current. The resistivity is $\rho_\perp$ in the whole sample. From A to B, the resistance is kept unchanged because the saturated state is maintained. Then, when the magnetic field reaches H_{n1}, the resistance increases sharply and reaches its maximum value at C. At this point, the magnetic moments located in the domain wall [Fig. 5(c)] are no longer perpendicular to the electrical current and they exhibit a parallel component. The magnetic moments of a layer confined between x and $x+dx$ form a $\theta(x)$ angle with the current flow that is along $0y$. Each layer contributes to the total electrical resistance of the sample with the resistivity $\rho(\theta)$. From C to D, the electrical resistance decreases slowly because of the compression of the domain wall against the TbFe layer. The reason of the decrease of the resistance is that the compression leaves less and less spins in the direction of the electrical current. At the propagation field $H_p(T)$, which in the GdFe (1000 Å)/TbFe(15 Å)/GdFe(500 Å) is close to 50 Oe at $T=60$ K, the domain wall crosses the barrier, and after its traveling through the GdFe (500 Å) layer, all the magnetic moments become aligned along the direction of the magnetic field $-0z$ [Fig. 5(f)]. They are again perpendicular to the electrical current [point E, Fig. 4(c)]. As in zero field, the resistivity is uniformly $\rho_\perp$ and the resistance recovers its minimal value. The cycling of the field leads to a symmetrical behavior about the vertical axis of Fig. 7(a).

From resistance measurements performed on a second sample in the parallel geometry (we could not use the same sample because the electrodes had to be placed differently), we found that the electrical variations were opposite and symmetrical about the horizontal axis of Fig. 7(a). There is a drop of the resistance at H_{n1}, a slow increase between H_{n1} and H_p, and a sharp increase at the field H_p beyond which the initial resistance is recovered. In this geometry, all the magnetic moments are parallel to the electric current when there is no domain wall (the resistance is the highest) and a part of them are perpendicular to the electric current, when a domain wall is present. In that sample, the compression of the domain wall manifests by a slow increase of the resistance.

C. Double nucleation and annihilation

A second set of resistance curves obtained in the transverse configuration shows, at 30 K [Fig. 7(b)], both the double nucleation and the annihilation processes. On that curve, the points A, B, C, and D represent similar situations as in curve 7(a). From A to B, the magnetization is uniform along the cooling field and is perpendicular to the electrical current. The step B-C corresponds to the nucleation of the domain wall in the thicker GdFe layer. From C to D, the resistance decreases slowly because the domain wall, nucleated at H_{n1}, compresses against the TbFe layer [Fig. 5(c)]. However, beyond D, the evolution of the resistance turns out to be different. First of all, there is a second step D-F, which corresponds to the nucleation of the second domain wall in the GdFe (500 Å) layer [Fig. 5(d)]. With two domain walls, more magnetic moments exhibit a component along the electric current and as a consequence, the electrical resistance is still higher. From F to G, the resistivity decreases slowly in the same way as between C and D, which is typical of the compression of domain walls: here, two domain walls are compressed simultaneously. Finally, beyond G, the resistivity decreases rapidly with the reverse of the magnetization of the TbFe layer and the annihilation of the domain walls. Again, the cycling of the field gives symetrical curves about the vertical axis of the figure.

As at 60 K, the transverse resistivity measurements performed on a second sample where the electrodes had been placed appropriately exhibit opposite curves. The steps of increase of resistivity are replaced by steps of decrease,

which once more supports the interpretation of the data by the mechanism of magnetoresistance anisotropy.

D. Resistivity of a domain wall

Beyond the qualitative aspects developed above to understand the behavior of domain walls, it would be of interest to perform a quantitative analysis of the resistivity of one domain wall. It certainly requires more measurements from different samples in parallel and transverse geometry, to see for example if other electron scattering mechanisms are involved.[26–28] However, as the AMR is undoubtedly the dominant effect, a first simple analysis of the variation of the resistance with the domain-wall compression can be presented.

As it is well known, in a thin-film sample whose length (direction of the current flow) is L, whose width and thickness are w and e, respectively, and in which the resistivity is a function of x ($0x$ is the direction perpendicular to the plane of the sample), the resistance is given by

$$\frac{1}{R}=\frac{w}{L}\int_0^e \frac{dx}{\rho(x)}.$$

If the spatial variation of the resistivity is due to the orientation of the spins (AMR), which are supposed to be parallel to each other in the layer comprised between x and $x+dx$, but which rotate along the $0x$ direction, the resistivity is $\rho(x)=\rho_\perp+\Delta\rho\cos^2\theta(x)$. $\theta(x)$ is the angle between the direction of the spins and the electrical current. The resistance of the sample can be expressed by

$$\frac{1}{R}=\frac{w}{L}\frac{1}{\rho_\perp}\int_0^e \frac{dx}{1+\frac{\Delta\rho}{\rho_\perp}\cos^2[\theta(x)]}.$$

Let us now define a ''single domain-wall sample.'' It is a hypothetical sample in which a domain wall spreads from a surface of the sample ($x=0$) to the other one ($x=e=\delta$). In such a sample, the spins located on the first surface, at $x=0$, are parallel to the field direction. Those in contact with the second surface at $x=\delta$ are oriented antiparallel to the field. Between $x=0$ and $x=\delta$, we can assume that, as in a first approximate in domain walls,[29] the rotation varies linearly with x. Therefore, in the longitudinal geometry where the electrical current is parallel to the field, $\theta(x)=\pi x/\delta$. At the opposite, in the transverse geometry where the electrical current is perpendicular to the field: $\theta(x)=\pi/2-\pi x/\delta$.

As a result, because in both geometries the distribution of the spins spreads with an equal weight in all the directions of the space, the resistance of a ''single domain-wall sample'' of thickness δ is given by the same expression:

$$R^{\mathrm{DW}}(\delta)=\frac{\rho_\perp L}{w\delta}\sqrt{1+\frac{\Delta\rho}{\rho_\perp}}=\frac{L\sqrt{\rho_\perp\rho_\parallel}}{w\delta}.$$

If the sample is a GdFe/TbFe/GdFe trilayer where $e\ll e_1$ and e_2 and in which a domain wall of thickness δ has developed [see Fig. 5(c)], the total resistance $R_\perp(\delta)$ in the transverse geometry can be considered as the result of three resistances in parallel: the resistance of the domain wall of thickness δ, the resistance of the rest of GdFe layer whose thickness is $e_1-\delta$ and the GdFe layer. The resistivity of the last two parts is $\rho_\perp$.

This gives

$$\frac{1}{R_\perp(\delta)}=\frac{w(e_1+e_2-\delta)}{L\rho_\perp}+\frac{1}{R^{\mathrm{DW}}(\delta)},$$

or

$$\frac{1}{R_\perp(\delta)}=\frac{1}{R_\perp(0)}\left[1+\left(\frac{\delta}{e_1+e_2}\right)\left(\sqrt{\frac{\rho_\perp}{\rho_\parallel}}-1\right)\right]$$

with $\rho_\parallel>\rho_\perp$, $R_\perp(\delta)$ is an increasing function of δ. The nucleation of a domain wall produces a positive step of resistance, its disappearance a negative step and the domain-wall compression, a slow decrease of the resistance.

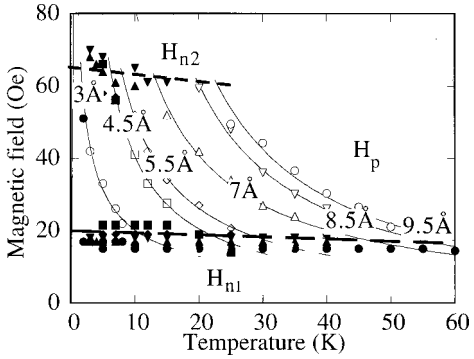

FIG. 8. Variation of the propagation field H_p as a function of the temperature for a selection of GdFe(1000 Å)/TbFe/GdFe(500 Å) samples. The values indicated on each curve correspond to the thickness of the TbFe layers.

V. DISCUSSION

In this section, we first present and discuss the thermal dependence of the propagation field $H_p(T)$ on the thickness of the TbFe layer. In the second part, we focus on the nucleation fields H_{n1} and H_{n2} and propose an estimate of these quantities. For this purpose, we use a very simple model derived from those which have been proposed to evaluate the exchange bias field in ferromagnet-antiferromagnet bilayers. We show that, in our system, as in exchange biased layered structures, a shift of the hysteresis loop appears. In the third part, we present an analysis of the compression and double-compression stages of the magnetization curves and evaluate the thickness of the compressed domain wall as a function of the applied magnetic field.

A. Thermal dependence of the propagation field

The propagation fields $H_p(T)$ deduced from a set of different GdFe(1000 Å)/TbFe/GdFe(500 Å) samples whose TbFe thicknesses were between 3 and 9.5 Å are plotted in Fig. 8. As it can be seen, the propagation fields are restricted to the range $\approx 20-60$ Oe. The reason is now obvious: the propagation fields can only be determined beyond the first nucleation field H_{n1} and below H_{n2}, the field at which the propagation is bypassed by the nucleation of a domain wall in the thinner GdFe layer.

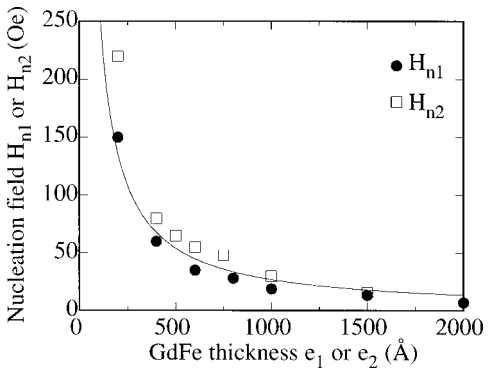

FIG. 9. Evolution of H_{n1}, the nucleation field in the GdFe(e_1), as a function of e_1 and of H_{n2}, the nucleation field in the GdFe(e_2), as a function of e_2.

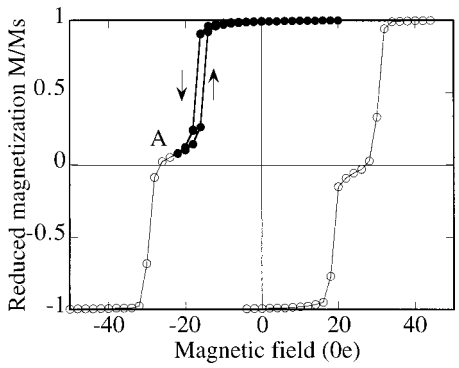

FIG. 10. Decompression of the domain wall in a GdFe(1000 Å)/TbFe(4.5 Å)/GdFe(500 Å) sample. The minor cycle has been obtained after reversing the field at point *A* in the compression stage.

At a given temperature T, the field to be applied for the crossing of the barrier increases with the thickness of the TbFe layer. On the other hand, under a given magnetic field, a larger temperature is required for the crossing of a thicker TbFe layer. From these observations, we can conclude that the height of the barrier increases with the TbFe thickness and that the crossing of the barrier is a thermally activated phenomenon.

B. Nucleation of the domain walls and exchange biasing problem

From a lot of samples prepared with different thicknesses e_1, e_2, and e, we have observed that the nucleation field H_{n1} depends actually only on the thickness e_1 of the layer in which the nucleation occurs. Likewise, the nucleation field H_{n2} depends mainly on e_2. It is important to note that H_{n1} and H_{n2} are independent of the TbFe layer thickness. H_{n1} and H_{n2} increase when e_1 and e_2, respectively, decrease and, as a matter of fact, $H_{n1}(e_1)$ and $H_{n2}(e_2)$ follow about the same curve (Fig. 9). Such a behavior can be easily understood if we consider that, in both cases, a domain wall is created against the TbFe layer whose magnetization is at first kept unchanged [Fig. 5(b)].

For the nucleation process, two energies have to be considered: (i) the Zeeman energy and (ii) the domain-wall energy. Consider (Fig. 5) the trilayer system submitted to the field H antiparallel to the cooling field, before the nucleation [Fig. 5(a)] and after the nucleation of the domain wall [Fig. 5(c)]. The occurrence of the domain wall lowers the Zeeman energy because of the complete reversal of the magnetization in the thickness $(e_1-\delta)$ and because of the semireversal of the magnetic moments of the domain wall. The variation of Zeeman energy per surface unit is $-2M_SH\ (e_1-\delta/2)$. On the other hand, the occurrence of the domain wall increases the energy by $\gamma=4\sqrt{AK}$. As a consequence, a critical field larger than $\gamma/2M_S(e_1-\delta)$ is required for the nucleation of a domain. With $e_1=1000$ Å, $\delta=700$ Å, $M=1400$ emu and $\gamma=0.35$ erg/cm^3, we find $H_{n1}=28$ Oe. The estimated value is of the right order of magnitude, even if this relation represents a first approximate. It has to be improved to take into account the fact that the shape of the domain wall is modified by the field and that γ and δ themselves depend on the magnetic field. However it clearly shows that the critical field H_{ni} $(i=1,2)$ increases when e_i decreases.

At this stage, we propose a parallel between the problem of nucleation in the GdFe layer with formation of domain wall against the TbFe layer and the exchange biasing problem, which is currently a subject of great interest.[30–32] The exchange biasing occurs in ferromagnetic-antiferromagnetic bilayers where the reversal of the magnetization of the ferromagnetic layer is accompanied by the occurrence of an interface energy. The exchange biasing field (that is actually close to our nucleation field) is the result of the balance between the Zeeman energy and the interface energy. It is usually given by $H_{EB}=\Delta\sigma/2M_Se$, where e is the thickness of the ferromagnetic layer and $\Delta\sigma$ is the interface energy. This relation assumes that the reversal of the magnetic moments of the ferromagnetic layer is complete and that the interface energy is rather localized in the antiferromagnetic layer, for example with the formation of a domain wall inside that layer.[33] In our system, where the soft antiferromagnetic layer is replaced by a very hard ferromagnetic layer, the interface energy $\Delta\sigma$ is simply the domain wall energy γ that is localized inside the soft magnetic material. The difference between the expressions of H_{EB} and H_{n1} stands in the substitution of e by $(e-\delta/2)$. The substraction of $\delta/2$ is due to the space occupied by the domain wall inside the GdFe(1000 Å) layer (instead of inside the antiferromagnetic layer in the ferromagnetic/antiferromagnetic bilayers).

Here, likewise in the exchange biasing problem, the domain wall acts as an elastic spring compressed by the magnetic pressure. When the magnetic field is lowered, the magnetic pressure is reduced and the energy stored in the domain wall is large enough to reverse the magnetization of the layer in the direction of the cooling field, even before the field returns to zero. As a consequence, in both cases, the hysteresis loop is shifted. Figure 10 shows the decompression effect which occurs in a GdFe(1000 Å)/TbFe(4.5 Å)/GdFe(500 Å) sample, when the field is reversed from point *A*, located before the propagation field. It appears as a minor cycle because only the magnetization of the GdFe(1000 Å) is concerned. During this cycle, the magnetization of the GdFe(500 Å) layer is unchanged.

C. Thickness and compression of the domain walls

We focus now on the compression of the domain walls against the TbFe layer. The thickness of the domain walls

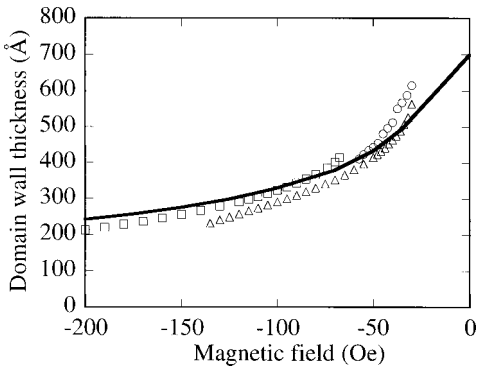

FIG. 11. Evolution of the thickness of the domain wall δ as a function of the applied magnetic field. Symbols are used to plot data determined from the experimental magnetization measurements: Circles: GdFe(1000 Å)/TbFe(9.5 Å)/GdFe(500 Å) at 5 K for 20 Oe$<H<$60 Oe in the compression domain. Triangles: GdFe(1000 Å)/TbFe(9.5 Å)/GdFe(200 Å) at 5 K for 20 Oe$<H<$140 Oe in the compression domain. Squares: GdFe(1000 Å)/TbFe(9.5 Å)/GdFe(500 Å) at 5 K for 70 Oe$<H<$200 Oe in the double compression-domain. The continuous line corresponds to a simulation of a linear chain of spins with $H_K=70$ Oe and $A=17$ 10^{-8} erg/cm.

and their compression are shown by the amplitudes of the magnetization steps that occur at H_{n1} and H_{n2} and by the slow decrease of the magnetization in the ''compression'' stage between H_{n1} and $H_p(T)$ or in the double-compression stage between H_{n2} and H_a. The first important point to consider for the evaluation of the thickness of the domain wall is the amplitude ΔM of the magnetization step at the nucleation field H_{n1}. Indeed, the reversal of the magnetization of the whole GdFe(e_1) layer at H_{n1} (without formation of domain wall), would produce a reduced magnetization step $\Delta M/2M_S=e_1/e_1+e_2$. After the step, the magnetization should be stabilized (up to H_{n2}) on a plateau at a reduced magnetization $M/M_S=(e_2-e_1)/(e_1+e_2)$. With $e_1=1000$ Å and $e_2=500$ Å, the magnetization plateau should be at $M/M_S=-0.33$. But, as seen in Figs. 4 and 6, the magnetization step which occurs at H_{n1} is significantly smaller. The missing part of amplitude of the step is due to the occurrence of the domain wall and to the fact that, in average, the variation of the magnetization of the spins involved in the domain wall is M_S instead of $2M_S$. The amplitude of the step becomes $\Delta M/2M_S=(e_1-\delta)/(2/e_1+e_2)$ and, between H_{n1} and H_p, the width of the domain wall is then related to the magnetization $M(H)$ by the relation $\delta(H)=M(H)[(e_1+e_2)+(e_1-e_2)]/M_S$. Therefore, the fact that in each sample where $e_1=1000$ Å and $e_2=500$ Å, M is equal to 0 at $H=35$ Oe, which means that for this field δ (35 Oe) is equal to 500 Å. The thickness of the domain wall is largely independent of the TbFe thickness and of the temperature.

Thus, from the field dependence of $M(H)$ in the ''compression'' stage and by using the above relation, we have deduced the field dependence of $\delta(H)$. In Fig. 11, we present the results obtained from the GdFe(1000 Å)/TbFe(9.5 Å)/GdFe(500 Å) sample.

Let us now come to the simultaneous compression of the two domain walls represented in Fig. 5(e), which occurs between H_{n2} and H_a. Such a double compression explains the slow decrease of the magnetization, as it occurs, for example, at 10 K, between 70 and 180 Oe in Fig. 6. If we assume that the two domain walls are identical on each side of the TbFe layer, their thicknesses are related to the magnetization by $\delta(H)=M(H)[(e_1+e_2)+(e_1-e_2)]/2M_S$. The values deduced from experimental data, by using this relation, are reported in Fig. 11. They are quite in agreement with the values deduced from a single compression.

Finally, the experimental width $\delta(H)$ has been compared with the wall thicknesses deduced from the simulation of a linear chain of spins (continuous line in Fig. 11), in which each spin is submitted to an external field H, to an uniaxial anisotropy K and interacts with its neighbors via an exchange constant A. In this simulation, the last spin of the chain was fixed antiparallel to the external field and the other ones were free. An agreement between experimental data and the simulation leads to an A value of about 17×10^{-8} erg/cm, which is quite consistent with the value deduced from the exchange constants given by Hansen *et al.*[10]

VI. CONCLUSION

With the GdFe(1000 Å)/TbFe/GdFe(500 Å) trilayer system, this paper reports on the elaboration of the domain-wall junction as suggested in a theoretical paper by Gunther and Barbara.[4] We first studied the conditions in which a domain wall could be nucleated in one of the GdFe layers and proposed an asymmetrical device with two different GdFe layer thicknesses. This disymmetry leads to two different nucleation fields H_{n1} and H_{n2} in the two GdFe(1000 Å) and GdFe(500 Å) layers, and leaves the 20–60 Oe magnetic-field range available to study the propagation of the domain wall nucleated in the GdFe(1000 Å). On the other hand, we showed that, when the propagation field H_p is ''virtually'' larger than 60 Oe, two domain walls were nucleated on each side of the TbFe layer and the propagation was bypassed.

The occurrence of the two domain walls has been established on one hand by the amplitude of the magnetization steps that occur at the nucleations, and on the other hand by the anisotropy of magnetoresistance that is related to the amount of magnetic moments along the directions parallel and perpendicular to the electrical current. From the magnetization data, we could determine the variation of the width of the domain walls as a function of the field in the compression as well as in the double-compression stage.

Then, we established that the height of the energy barrier due to the presence of the TbFe layer in GdFe/TbFe/GdFe increases with the TbFe thickness and that the crossing of the barrier was thermally activated. The height and the shape of the potential barrier as a function of the TbFe thickness and of the applied magnetic field is still to determine quantitatively. This is currently performed by relaxation measurements of the magnetization. On the other hand, it has been shown that at very low temperatures, a crossing of the barrier by the tunnel effect was possible.[34]

An important problem is the way the domain wall propagates through the TbFe layer. In fact, we suggest that, regarding Gunther and Barbara's analysis,[4] our system constitutes an unconventional domain-wall junction because of the sperimagnetic structure of the TbFe amorphous alloy and of the large random anisotropy of terbium in this amor-

phous alloy.[15] We believe that at H_p, under the pressure of the domain wall and because of the low temperature, the magnetization of the TbFe layer ''switches'' between two states. This is related to the shape of the hysteresis loops of the bulk TbFe amorphous alloy. In such systems with a strong random anisotropy, the loops are pretty square and are interpreted by the collective spin flop of spins along the local easy axis. In a recent simulation, Saslow and Koon[35] showed that half of the spin flips occured at the vicinity of the coercitive field. This means that the GdFe/TbFe/GdFe system could be analyzed in a different way and that an extended classification of the domain-wall junctions has to be considered.

An important feature of this system is the occurrence of a kind of ''exchange biasing field'' referred to here as nucleation field. It seems clear that a parallel between the exchange biasing and the domain-wall junction problems has to be made.

Finally, our system can be fruitfully considered for the study of the magnetoresistivity of the domain walls that is currently a field of intense interest. In our study, we used the anisotropy of magnetoresistance to get information on the magnetic configuration of the sample. We are currently studying the resistivity in detail to quantify the anisotropy of resistivity and determine if other fundamental magnetoresistivity mechanisms are involved and could be shown.

[1] D. Jiles, *Introduction to Magnetism and Magnetic Materials* (St. Edmundsbury, Great Britain, 1991).
[2] P. C. E. Stamp, Phys. Rev. Lett. **66**, 2802 (1991).
[3] E. M. Chudnovsky, O. Iglesias, and P. C. E. Stamp, Phys. Rev. B **46**, 5392 (1992).
[4] L. Gunther and B. Barbara, Phys. Rev. B **49**, 3926 (1994).
[5] G. Tatara and H. Fukuyama, Phys. Rev. Lett. **72**, 772 (1994).
[6] S. Mangin, C. Bellouard, G. Marchal, and B. Barbara, J. Magn. Magn. Mater. **165**, 13 (1997).
[7] G. S. Cargill, Solid State Phys. **30**, 227 (1975).
[8] R. J. Elliott, *Magnetic Properties of Rare Earth Metals* (Plenum, London, 1972).
[9] K. Moorjani and J. M. D. Coey, *Metallic Glasses* (Elsevier, New York, 1984).
[10] P. Hansen, C. Clausen, G. Much, M. Rosenkranz, and K. Witter, J. Appl. Phys. **66**, 756 (1989).
[11] C. Dufour and G. Marchal, Rev. Sci. Instrum. **62**, 2984 (1991).
[12] Ph. Mangin, G. Marchal, C. Mourey, and Chr. Janot, Phys. Rev. B **21**, 3047 (1980).
[13] R. W. Cochrane, R. W. Harris, and M. J. Zuckermann, Phys. Rep. **1**, 1 (1978).
[14] M. Vaezzadeh, B. George, and G. Marchal, Phys. Rev. B **50**, 6113 (1994).
[15] E. C. Stoner and E. P. Wohlfarth, IEEE Trans. Magn. **MAG-27**, 3475 (1991).
[16] M. S. Cohen, in *Handbook of Thin Film Technology*, edited by L. Maissel and R. Glang (McGraw-Hill, New York, 1983), Chap. 17.
[17] S. Mangin, C. Bellouard, G. Marchal, and B. Barbara, J. Magn. Magn. Mater. **165**, 161 (1997).
[18] H. Ono, M. Ishida, M. Fujinaga, H. Shishido, and H. Inaba, J. Appl. Phys. **74**, 5124 (1993).
[19] R. Hasegawa, J. Appl. Phys. **45**, 3109 (1989).
[20] Y. Mimura, N. Imamura, T. Kobayashi, A. Okada, and Y. Kushiro, J. Appl. Phys. **49**, 1208 (1978).
[21] G. S. Cargill, AIP Conf. Proc. **18**, 631 (1974).
[22] L. A. Campbell and A. Fert, in *Ferromagnetic materials*, edited by E. P. Wohlfarth (North-Holland, Amsterdam, 1982), Vol. 3.
[23] J. Smit, Physica (Amsterdam) **16**, 612 (1951).
[24] A. Fert, Thèse Etat Orsay-France, 1970.
[25] M. Vaezzadeh, Thèse Université Nancy, France, 1993.
[26] M. Viret, D. Vignoles, D. Cole, W. Allen, D. S. Daniel, and J. F. Gregg, Phys. Rev. B **53**, 8464 (1996).
[27] J. F. Gregg, W. Allen, K. Ounadjela, M. Viret, M. Hehn, S. M. Thomson, and J. M. D. Coey, Phys. Rev. Lett. **77**, 1580 (1996).
[28] G. Tatara and H. Fukayama, Phys. Rev. Lett. **78**, 3773 (1997).
[29] A. Herpin, *Théorie du magnétisme Bibliothèque des Sciences et techniques Nucléaires* (Presses Universitaires de France, Paris, 1968).
[30] N. C. Koon, Phys. Rev. Lett. **78**, 4865 (1997).
[31] R. Jungblutt, R. Coehroorn, M. T. Johnson, J. aan de Stegge, and A. Reinders, J. Appl. Phys. **75**, 6659 (1994).
[32] D. Mauri, H. C. Siegmann, P. S. Bagus, and E. Kay, J. Appl. Phys. **62**, 3047 (1987).
[33] A. P. Malozemoff, J. Appl. Phys. **63**, 3874 (1988).
[34] S. Mangin, G. Marchal, W. Wernsdorfer, A. Sulpice, K. Hasselbach, D. Mailly, and B. Barbara, Europhys. Lett. **39**, 675 (1997).
[35] W. M. Saslow and N. C. Koon, Phys. Rev. B **49**, 3386 (1994).